IEEE Access
Multidisciplinary ⋮ Rapid Review ⋮ Open Access Journal

Received November 28, 2018, accepted December 10, 2018, date of publication February 25, 2019, date of current version March 7, 2019.

Digital Object Identifier 10.1109/ACCESS.2018.2886657

Synthesis of Dual-Band Bandpass Filters With Short-Circuited Multiconductor Transmission Lines and Shunt Open Stubs

JUAN JOSÉ SÁNCHEZ-MARTÍNEZ, MARIO PÉREZ-ESCRIBANO, (Student Member, IEEE), AND ENRIQUE MÁRQUEZ-SEGURA, (Senior Member, IEEE)

Departamento de Ingeniería de Comunicaciones, Escuela Técnica Superior de Ingeniería de Telecomunicación, Universidad de Málaga, 29071 Málaga, Spain

Corresponding author: Mario Pérez-Escribano (mpe@ic.uma.es)

This work was supported in part by the Spanish Ministerio de Economía, Industria y Competitividad, under Project ADDMATE TEC2016-76070-C3-3-R (AEI/FEDER, UE), in part by the Spanish Ministerio de Educación, Cultura y Deporte, under Grant FPU16/00246, and in part by Universidad de Málaga, under I Plan Propio de Investigación y Transferencia (C.1).

ABSTRACT The design of dual-band bandpass filters consisting of series short-circuited wire-bonded multiconductor transmission lines and shunt open stubs is thoroughly carried out in this paper. Two different configurations are studied, and closed-form analytical design equations are derived to synthesize Chebyshev filtering functions. A novel, simplified, and time-saving synthesis procedure to design dual-band filters with narrow or moderate broad bandwidths is finally presented, attending to the required final specifications and the physical and manufacturing limitations. The usefulness and validity of the proposed analytical equations are illustrated by designing, manufacturing, and measuring three different prototypes, showing an excellent agreement between analytical and measured results.

INDEX TERMS Bandpass filter, Chebyshev response, coupled lines, dual-band, multiconductor transmission lines (MTLs), shunt stubs.

I. INTRODUCTION

Nowadays, the enormous growth of data traffic is promoting new solutions which are used to transport this high amount of data. To satisfy this demand, different techniques, such as multiple-input-multiple-output systems, multicarrier, or carrier aggregation, are used. Nevertheless, not only signal processing is important to achieve high data rates, but also every part of the communication system can be enhanced. In the RF domain, there are many improvements that are utilized, such as the use of wider, double, triple band systems [1], [2]. In this sense, bandpass filters are one of the most important components, and multiband responses have become essential in the design of RF circuits [3], [4].

The main issue of double band filters is that they must be designed and optimized for diverse specifications and applications, which could need broad or narrow bandwidths, large or small frequency ratios and different in-band ripple factors or return losses. Different topologies have been proposed to achieve these specifications. The most straightforward ways of designing dual-band filters is by cascading two single-band filters [5] or combining a wideband filter with a bandstop filter [6]. These methods are the simplest, but they usually have problems with insertion losses and circuit size. For that reason, the main topologies proposed by researches are based on multimode resonator. These filters can be implemented in different shapes and topologies, including open loop resonators [7], [8], ring resonators [9], [10], stepped-impedance resonators [11], [12] or quadruple-mode resonators [13]. Furthermore, the coupling between adjacent resonators is normally complicated, and there is a strong dependence on full-wave simulations to characterize it. Therefore, the time spent in the design and optimization process of filters based on resonators is usually large. Transmission or coupled lines are also quite used in planar dual-band bandpass filters, both in single-layer [14], [15] as in multilayer technologies [16], [17]. Under certain conditions, as proposed in this paper, it is possible to obtain analytical design expressions, even without the use of electromagnetic simulators. Apart from that, mathematical transformations from single-band to multiband filters have been proposed, in order to synthesize multifrequency responses from single ones [18].

2169-3536 © 2019 IEEE. Translations and content mining are permitted for academic research only.
Personal use is also permitted, but republication/redistribution requires IEEE permission.
See http://www.ieee.org/publications_standards/publications/rights/index.html for more information.

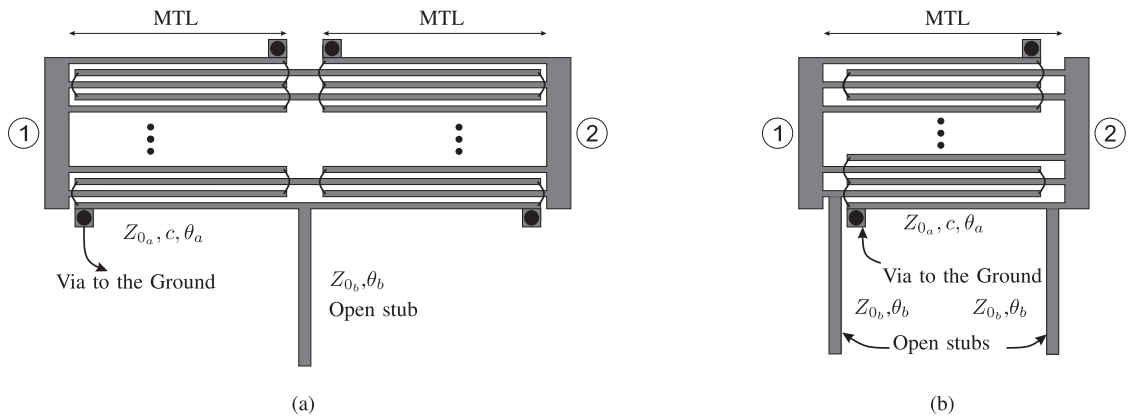

FIGURE 1. Layout of the proposed circuit for the analyzed dual-band bandpass filters: (a) prototype I and (b) prototype II.

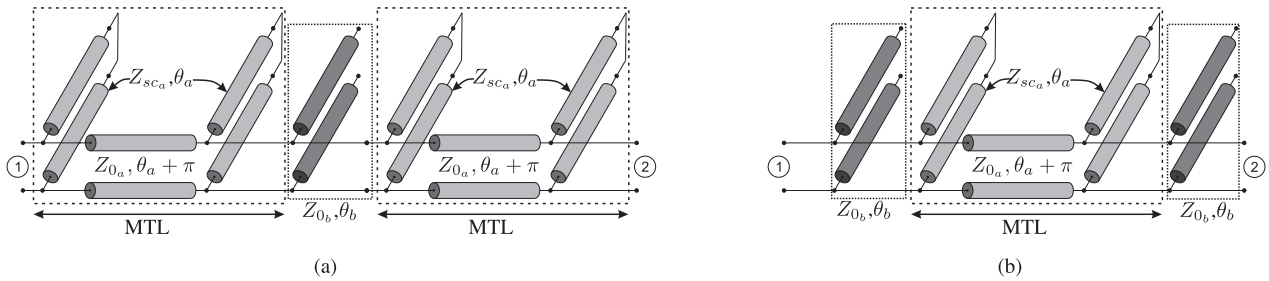

FIGURE 2. Equivalent circuit model for the proposed filters: (a) prototype I and (b) prototype II.

In this work, two topologies of dual-band planar bandpass filters based on series short-circuited multiconductor transmission lines (MTLs) and shunt open stubs are proposed and analyzed through analytical equations. Previously, one of these had been used by Pérez-Escribano *et al.* [19] for a design, without making a deep analysis. By using the proposed architectures, dual-band filters with one or two poles in each band can be achieved. As one of the main contributions, new design equations to synthesize filters with a Chebyshev-type response by means of a quick and reliable procedure are deduced.

This paper is structured as follows. First, in Section II-A, a circuit analysis of the two presented topologies is carried out, in order to characterize the behavior of both topologies separately. Subsequently, dual-band filtering functions and a transformation between frequency and electric length domains are presented in Section II-B. By using such transformations, a synthesis procedure and a complete set of analytical equations for the design of Chebyshev-type dual band filters are obtained in Section II-C. A design methodology, taking into account the limitations of the filter, is proposed in Section III. Finally, in Section IV, an experimental validation is carried out, by designing, fabricating, and measuring three filters, corroborating the developed theory and techniques. Conclusions are given in the last section.

II. ANALYTICAL DESIGN PROCEDURE

In this work, two circuit topologies, shown in Fig. 1, have been analyzed. The procedure used to analyze these circuits is similar to the one in [20]–[24]. Firstly, the frequency response of the circuits is computed (i.e., the S_{21} parameter). Then, a proper filtering function for synthesizing dual-band band pass filters (BPFs) is obtained, and finally, the circuit design parameters are determined by equating the transfer functions to the filtering functions. By means of this procedure, closed-form analytical design equations are obtained to design dual-band BPFs with known return losses and operating bandwidths.

A. CIRCUIT ANALYSIS

The proposed circuits (see Fig. 1) are composed of series short-circuited MTLs and shunt open-circuited stubs. Two symmetrical prototypes are considered in order to design first- and second-order dual-band BPFs. The analysis of both filters can be directly carried out by using the equivalent circuit for a short-circuited MTL [25], consisting of a transmission-line section and two shunt short-circuited stubs with characteristic impedances Z_{0_a} and Z_{sc_a}, respectively. The equivalent circuit models based on transmission-line for both prototypes are depicted in Fig. 2. On the one hand, the characteristic impedances of the MTL, Z_{0_a} and Z_{sc_a}, are given by

$$Z_{0_a} = \frac{2}{(k-1)(Y_{oo} - Y_{oe})} = \frac{2Z_{oe}Z_{oo}}{(k-1)(Z_{oe} - Z_{oo})} \tag{1a}$$

$$Z_{sc_a} = Z_{oe}\left(1 + \frac{(k-2)Z_{oo}}{Z_{oe} + Z_{oo}}\right)^{-1} = Z_{0_a}\frac{c}{1-c}, \tag{1b}$$

where Z_{oe} and Z_{oo} denote the even- and odd-mode impedances of a pair of coupled lines and k is the number of conductors. θ_a is the electrical length of a MTL, computed as the arithmetic mean value of the even- and odd-mode electrical lengths, and c is related to the maximum coupling coefficient of a k-lines quarter-wavelength four-port coupler [26], which can be written as

$$c = \frac{Z_{oe} - Z_{oo}}{Z_{oe} + Z_{oo}} \left(1 - \frac{(k-2)2Z_{oe}Z_{oo}}{(k-1)(Z_{oe}+Z_{oo})^2}\right)^{-1}. \quad (2)$$

On the other hand, the open-circuited stubs are defined by their characteristic impedance Z_{0_b} and their electrical length θ_b.

To analyze these circuits the even- and odd-mode analysis is employed. Once the even- (Z_{in_e}) and odd-mode (Z_{in_o}) input impedances are calculated, the S-parameters of the filters are determined as

$$S_{11} = \frac{Z_{in_e}Z_{in_o} - Z_0^2}{\Delta}, \quad S_{21} = \frac{Z_0\left(Z_{in_e} - Z_{in_o}\right)}{\Delta}$$
$$\Delta = Z_0^2 + Z_0\left(Z_{in_e} + Z_{in_o}\right) + Z_{in_e}Z_{in_o}, \quad (3)$$

being Z_0 the characteristic impedance used to terminate the input and output ports. These expressions can be simplified because both, the wire-bonded MTL and the open stubs, are chosen to be a quarter-wavelength long at the middle frequency (f_o) of the desired two passbands. Besides, assuming a TEM propagation, it can be considered that

$$\theta_a = \theta_b = \theta = \theta_o \frac{f}{f_o} = \frac{\pi}{2}\frac{f}{f_o}. \quad (4)$$

From (3) and after some algebraic transformations, the squared magnitude of S_{11} and S_{21} can be expressed as

- Prototype I

$$|S_{11}|^2 = \frac{F_I^2}{1+F_I^2}, \quad |S_{21}|^2 = \frac{1}{1+F_I^2} \quad (5a)$$
$$F_I = \frac{g_4 \tan^4\theta + g_2 \tan^2\theta + g_0}{\tan\theta\left(1+\tan^2\theta\right)} \quad (5b)$$
$$K_I = \frac{1}{2c^3\bar{Z}_{0_a}\bar{Z}_{0_b}} \quad (5c)$$
$$g_4 = \bar{Z}_{0_a}^3 c^3 K_I \quad (5d)$$
$$g_2 = \left(\bar{Z}_{0_a}c + 2\bar{Z}_{0_b}c^2\left(1-\bar{Z}_{0_a}^2\right)\right)K_I \quad (5e)$$
$$g_0 = -2\bar{Z}_{0_b}\left(1-c^2\right)K_I \quad (5f)$$

- Prototype II

$$|S_{11}|^2 = \frac{F_{II}^2}{1+F_{II}^2}, \quad |S_{21}|^2 = \frac{1}{1+F_{II}^2} \quad (6a)$$
$$F_{II} = \frac{p_4 \tan^4\theta + p_2 \tan^2\theta + p_0}{\tan^2\theta\,(1/\sin\theta)} \quad (6b)$$
$$K_{II} = \frac{1}{2c^2\bar{Z}_{0_a}\bar{Z}_{0_b}^2} \quad (6c)$$
$$p_4 = \bar{Z}_{0_a}^2 c^2 K_{II} \quad (6d)$$
$$p_2 = -\left(2\bar{Z}_{0_a}\bar{Z}_{0_b}c + \bar{Z}_{0_b}^2 c^2\left(1-\bar{Z}_{0_a}^2\right)\right)K_{II} \quad (6e)$$
$$p_0 = \bar{Z}_{0_b}^2\left(1-c^2\right)K_{II} \quad (6f)$$

where

$$\bar{Z}_{0_a} = Z_{0_a}/Z_0, \quad \bar{Z}_{0_b} = Z_{0_b}/Z_0. \quad (7)$$

The frequency response of both structures is perfectly characterized by means of (5) and (6), and taking into account the form of F_I and F_{II}, designing dual-band bandpass filters with real transmission zeros at $\theta_z = z\frac{\pi}{2}$ and $z = 0, 1, 2, \ldots$ is possible. These transmission zeros are used to enhance both, the isolation between two pass-bands and the rejection level in the lower and upper stop-bands. The transmission zeros at $\theta_z = z\frac{\pi}{2}$, $z = 0, 2, 4, \ldots$ are inherent to the series MTL while the zeros at $\theta_z = z\frac{\pi}{2}$, $z = 1, 3, \ldots$ are caused by the open stubs. Moreover, because of the degree of the numerator of F_I and F_{II} is four, both structures are, a priori, suitable to synthesize fourth-order dual-band band-pass filters. By adding different electrical length stubs, it could be possible to obtain multiband bandpass responses, forcing zeros in the MTL passband. Notwithstanding, this feasibility will depend on the physical realizability of the required values of Z_{0_a}, Z_{0_b} and c, which also conditions the operating bandwidths and the pass band frequency ratio.

Therefore, at this point it is important to highlight the advantages of using multiconductor transmission lines instead of only a pair of coupled lines. The achievable values of Z_{0_a} and c as a function of the line width W and spacing S for several number of conductors k are shown in [27]. These curves were calculated by using the Rogers 4350B substrate with a dielectric constant of 3.66 and thickness of 30 mils. This substrate will be used throughout the rest of this work. It is straightforward to observe that by increasing the number of conductors it is possible to reduce the value of Z_{0_a} with higher coupling values (c), which can be directly translated into wider bandwidths and higher frequency pass bands ratios. This behavior will be examined in Section III.

B. DUAL-BAND FILTERING FUNCTIONS

Given the transfer functions of the two configurations analyzed (5), (6), it is necessary to compute adequate filtering functions to properly synthesize the dual-band frequency responses. These functions have to be symmetric with respect to the middle design frequency f_o, with one or two transmission zeros at $\theta = \theta_0 = \pi/2$. Two procedures are explored to calculate such filtering functions. The first one uses a classical low-pass Chebyshev prototype [28], [29] with a dual-band frequency transformation (Fig. 3(a)) [18], [30], while the latter makes use of a generalized Chebyshev prototype [31] with the well-known Richard's transformation (Fig. 3(b)) [22]. Nevertheless, it is important to know the limitations or particularities of both methodologies. By using the first method, a dual-band filter of order $2m$ will have m coincident transmission zeros in the middle of the two pass bands (θ_0), while by means of the generalized Chebyshev

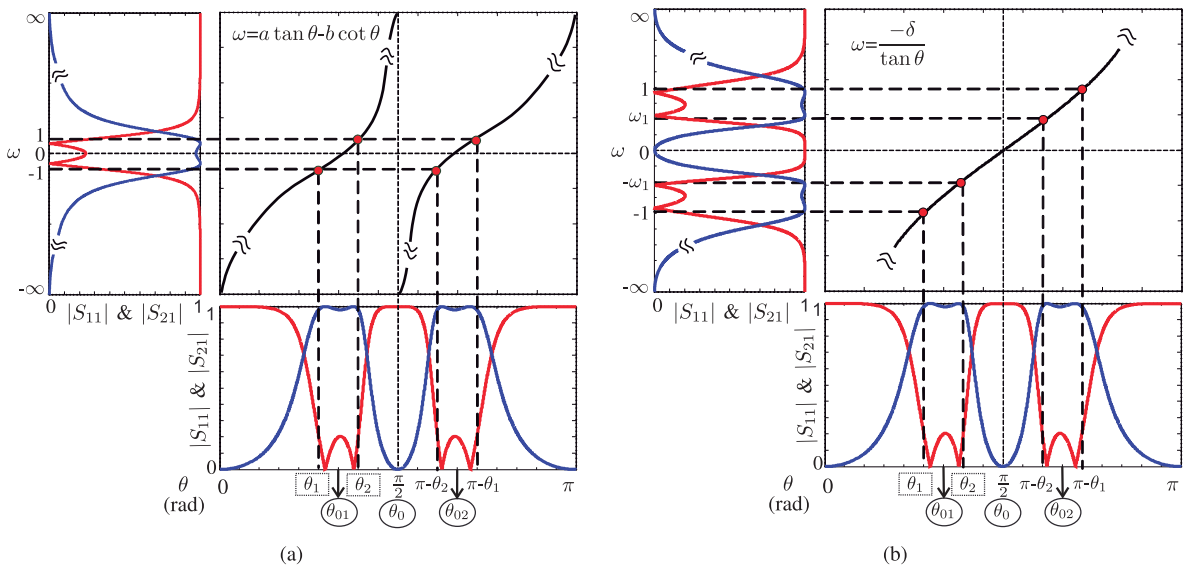

FIGURE 3. Transformations from the normalized ω-plane to the θ-plane using a (a) conventional low-pass Chebyshev prototype or (b) a generalized Chebyshev polynomial.

prototype, the number of zeros at θ_0 will be one or an odd number.

As seen in Fig. 3, the filtering functions in the normalized frequency ω corresponds to a conventional low-pass prototype (Fig. 3(a)) or a filter with two pass bands symmetrical respect to $\omega = 0$ (Fig. 3(b)). θ_1, θ_2, π-θ_2 and π-θ_1 relate to the lower and upper cut-off frequencies of the two pass bands with central frequencies given by θ_{01} and θ_{02} (being $\theta_{02} = \pi$-θ_{01}). By considering the desired fractional bandwidth of the first band (FBW) and the central frequencies of the dual pass bands (f_{01}, f_{02}), the required design parameters θ_1 and θ_2 are obtained as

$$f_o = \frac{f_{01}+f_{02}}{2}, \quad \text{FBW} = \frac{f_2-f_1}{f_{01}} = \frac{\theta_2-\theta_1}{\theta_{01}},$$
$$\theta_0 = \pi/2, \quad \theta_{01} = \frac{\pi}{2}\frac{f_{01}}{f_o},$$
$$\theta_1 = \theta_{01}\left(1-\frac{\text{FBW}}{2}\right), \quad \theta_2 = \theta_{01}\left(1+\frac{\text{FBW}}{2}\right), \quad (8)$$

and the frequency transformations are calculated as

- Conventional low-pass Chebyshev prototype [28] to dual-band BPF

$$\omega = a\tan\theta - b\cot\theta \quad (9a)$$
$$a = \frac{1}{\tan\theta_2-\tan\theta_1}, \quad b = \frac{\tan\theta_1\tan\theta_2}{\tan\theta_2-\tan\theta_1} \quad (9b)$$

- Generalized low-pass Chebyshev prototype [31] to dual-band BPF

$$\omega = \frac{-\delta}{\tan\theta}, \quad \delta = \tan\theta_1, \quad \omega_1 = \frac{\tan\theta_1}{\tan\theta_2}. \quad (10)$$

C. SYNTHESIS OF DUAL-BAND BANDPASS FILTERS

Once the transfer functions of the structures analyzed have been derived in Section II-A and the low-pass to dual-band bandpass frequency transformations are known (9), (10), the proper filtering functions are derived herein. Thus, the design parameters Z_{0_a}, Z_{0_b} and c can be easily calculated equating the transfer function of the circuits (F_I, F_{II}) to the theoretical filtering functions (F_n) as

$$\epsilon F_n(\theta) = F_{I,II}(\theta), \quad (11)$$

where ϵ is the in-band ripple factor related to a given return losses L_R in decibels as [32]

$$\epsilon = \frac{1}{\sqrt{10^{L_R/10}-1}}. \quad (12)$$

1) PROTOTYPE I

This prototype (Fig. 1(a)) has a polynomial F_I of order four with one real transmission zero at $\theta = \pi/2$, and thus, its frequency response can be modeled by using the generalized fourth-order Chebyshev function [31] and the Richard's frequency transformation. The transmission zeros of the S_{21} are located in

$$\tan\theta = 0, \infty; \quad \tan\theta = \pm j, \quad (13)$$

which can be mapped to the normalized ω frequency as (10)

$$\omega_{z1} = 0, \quad \omega_{z2} = \infty, \quad \omega_{z3,z4} = \pm j\delta = \pm j\tan\theta_1. \quad (14)$$

To compute the filtering function in the ω-plane, once the transmission zeros and the specifications of the pass bands (θ_1 and θ_2) are given, the recursive formulas derived in [31] are employed. Then, a filtering function for a fourth-order dual-band bandpass filter can be obtained. However, it can be

demonstrated that, regardless of the values of Z_{0_a}, Z_{0_b} and c, it is not possible to obtain four real transmission poles. The roots of the numerator of F_I can be calculated by solving the quadratic equation

$$g_4x^2 + g_2x + g_0 = 0, \tag{15}$$

with x $= \tan^2\theta$. However, because g_0/g_4 is always negative, one root of (15) will be positive whilst the other negative and, consequently, this structure is unsuitable to generate four real poles. Nevertheless, under the condition $\bar{Z}_{0_a}c = 1$, this topology can be used to design second-order dual-band BPFs. Imposing this relationship on (5), the new transfer function reduces to

$$\begin{aligned} F_I &= \frac{g_2\tan^2\theta + g_0}{\tan\theta}, \quad K_I = \frac{1}{2c^2\bar{Z}_{0_b}} \\ g_2 &= K_I, \quad g_0 = -2\bar{Z}_{0_b}\left(1-c^2\right)K_I. \end{aligned} \tag{16}$$

Note that this transfer function has only a transmission zero at $\theta = \pi/2$ and, thus, the dual-band filtering function F_n can be obtained using the two frequency transformations discussed in Section II-B. It can be proved that both methods lead to the same result. From a first-order Chebyshev polynomial in the ω-plane ($F_n = \omega$) and after the frequency mapping (9) to the bandpass domain, the filtering function is given by

$$\begin{aligned} F_n(\theta) &= \frac{g_{2t}\tan^2\theta + g_{0t}}{\tan\theta} \\ g_{2t} &= a, \quad g_{0t} = -b. \end{aligned} \tag{17}$$

Equating (17) to (16) the following relations between coefficients are obtained

$$\frac{g_0}{g_2} = \frac{g_{0t}}{g_{4t}}, \quad \epsilon = \frac{g_2}{g_{4t}}, \tag{18}$$

that can be used to calculate the closed-form design equations as

$$\bar{Z}_{0_b} = \frac{1+b\epsilon}{2a\epsilon} \tag{19a}$$

$$c = \frac{1}{\sqrt{1+b\epsilon}} \tag{19b}$$

$$\bar{Z}_{0_a} = 1/c. \tag{19c}$$

For this configuration there is a single transmission pole in each pass band, so that ϵ determines the return losses (L_R) at the cut-off frequencies (θ_1 and θ_2). Mathematical development of filtering functions for prototype I is described in Appendix A.

2) PROTOTYPE II

This prototype (Fig. 1(b)) has two real transmission zeros at $\theta = \pi/2$ (6b) and it can be designed to generate four real poles. Therefore, the use of a conventional second-order Chebyshev polynomial with the frequency transformation indicated in (9) is used to obtain the required theoretical filtering function. If the generalized Chebyshev low-pass prototype presented in [31] was used, it would be possible to generate only an odd number of transmission zeros at the middle frequency of the two pass bands. However, with the second-order polynomial and the low-pass to dual band-pass transformation (9), a filtering function with two real transmission zeros can be generated. The second-order Chebyshev polynomial $F_n = 2\omega^2 - 1$ is mapped to the θ-plane as

$$\begin{aligned} F_n(\theta) &= \frac{p_{4t}\tan^4\theta + p_{2t}\tan^2\theta + p_{0t}}{\tan^2\theta} \\ p_{4t} &= 2a^2, \quad p_{2t} = -(4ab+1), \quad p_{0t} = 2b^2, \end{aligned} \tag{20}$$

and by equating this function with (6b), the following relationships are derived

$$\frac{p_2}{p_4} = \frac{g_{2t}}{g_{4t}}, \quad \frac{p_0}{p_4} = \frac{g_{0t}}{g_{4t}}, \quad \epsilon = \frac{p_4}{p_{4t}}. \tag{21}$$

Note that the term $1/\sin\theta$ in (6b) is not in the filtering function obtained in (20). Therefore, the next design equations will provide an approximated synthesis procedure. Nevertheless, once the design parameters are obtained, they can be easily corrected by means of (6). From (21), the circuit design parameters can be calculated as

$$\bar{Z}_{0_a} = \left(1 + \frac{4ab\sqrt{1-c^2} - (4ab+1)(1-c^2)}{2b^2c^2}\right)^{\frac{1}{2}} \tag{22a}$$

$$\bar{Z}_{0_b} = \bar{Z}_{0_a}\frac{c}{\sqrt{1-c^2}}\frac{b}{a} \tag{22b}$$

$$\epsilon = \frac{1-c^2}{c^2}\frac{1}{4\bar{Z}_{0_a}b^2}, \tag{22c}$$

where $\bar{Z}_{0_a}$ and $\bar{Z}_{0_b}$ depend on both, the coupling factor and the specifications of the pass bands (θ_1 and θ_2). Besides, from (22a) and (22c) it is possible to find an expression that relates c with the in-band ripple factor ϵ (12) as

$$\begin{aligned} a_4x^4 + a_3x^3 + a_2x^2 + a_1x + a_0 &= 0 \\ a_4 &= 1 - 8\epsilon^2m^2b^2(1+4ab+2b^2) \\ a_3 &= 32\epsilon^2m^2ab^3 \\ a_2 &= 8\epsilon^2m^2b^2(1+4ab+4b^2) \\ a_1 &= -32\epsilon^2m^2ab^3 \\ a_0 &= -16\epsilon^2m^2b^4 \\ m &= 1/\sin\theta_{01} \end{aligned} \tag{23}$$

where

$$c = \sqrt{1-x^2}. \tag{24}$$

In (23) the term $\sin\theta_{01}$ has been included to compensate for the effect of $1/\sin\theta$. By means of this correction, it is guaranteed that the desired return losses are achieved at the central frequency of both pass bands. The analytical solution of this quartic equation (23), using an efficient algorithm proposed in [33], is described in Appendix B.

Consequently, once the specifications of the dual-band bandpass filter are known, equations (22a) and (22b) can be used along with (23) to determine the design parameters of the filter.

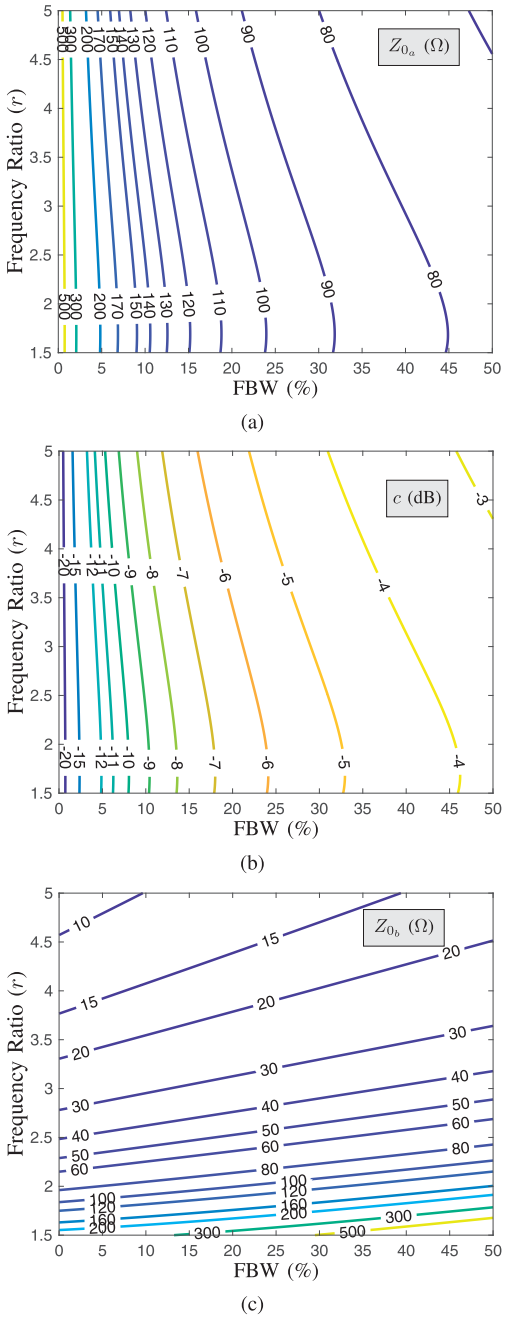

FIGURE 4. Z_{0_a}, c and Z_{0_b} values for prototype I, depending on the fractional bandwidth (FWB) and the frequency ratio (r), calculated using (19).

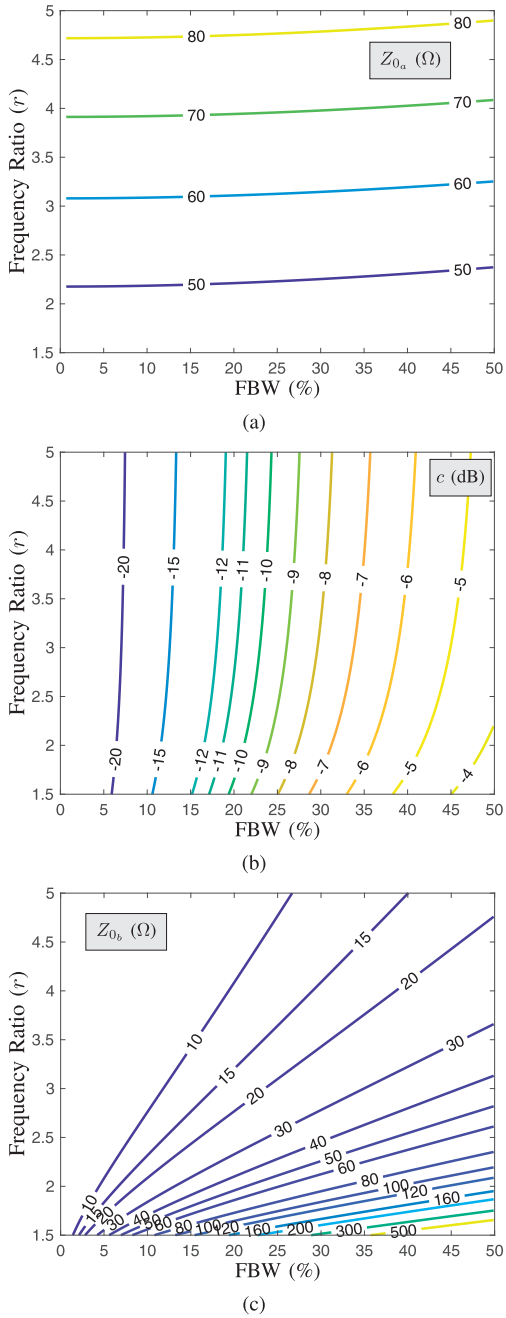

FIGURE 5. Z_{0_a}, c and Z_{0_b} values for prototype II, depending on the fractional bandwidth (FWB) and the frequency ratio (r), calculated using (22) and (24).

III. BANDWIDTH AND DESIGN CONSIDERATIONS

In the previous section, design equations for the two prototypes shown in Fig. 2 are obtained. However, it would be desirable to get a relation between the circuit design parameters and both, the achievable operating bandwidth and the pass band frequency ratio. Obviously, the performance of both filters will be conditioned by the required design values for the MTL and the shunt stub, and the limit values imposed by the manufacturing process capability. Therefore, depending on the obtained values, it is possible to establish some design criteria. Figures 4 and 5 show several values of Z_{0_a}, c and Z_{0_b} in order to achieve different combinations of fractional bandwidth (FBW) and frequency ratio ($r = f_{02}/f_{01}$) for prototypes I and II, respectively. $L_R = 3$ dB ($\epsilon = 1$) is used for prototype I, while for prototype II $L_R = 15$ dB has been employed. Thus, the 3 dB-fractional bandwidth is considered for the former, while the fractional bandwidth with equal-ripple response is defined for the latter. This definition is shown in Fig. 6.

As seen in Fig. 4, prototype I allows narrower bandwidths, independently of the separation between bands.

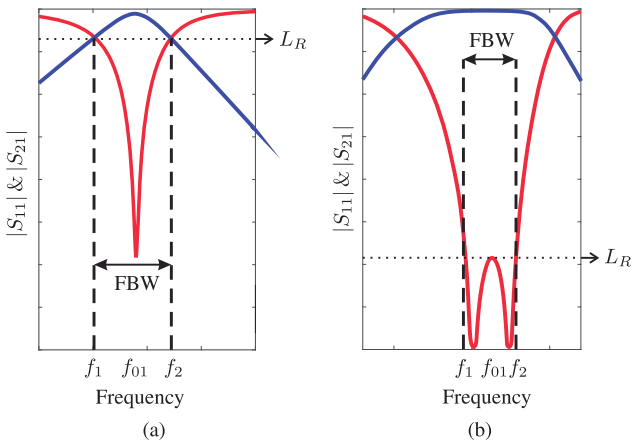

FIGURE 6. Fractional Bandwidth definition: (a) prototype I and (b) prototype II.

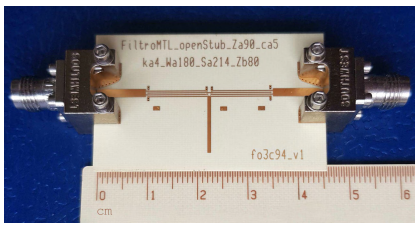

FIGURE 7. Photograph of the first prototype filter with connectors and a ruler that show its dimensions.

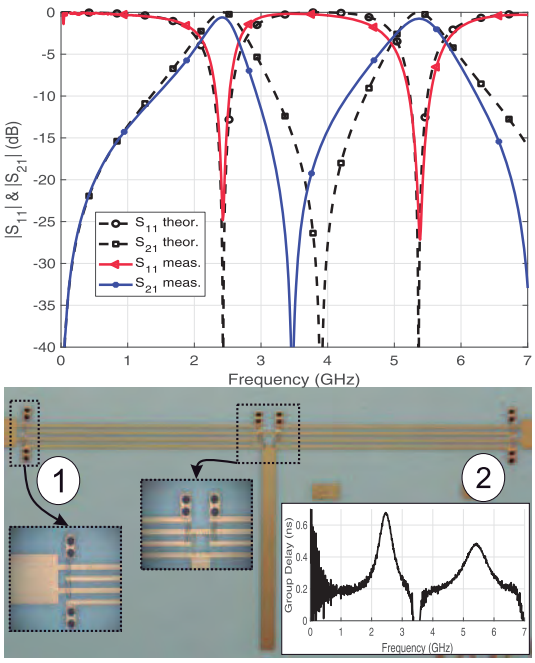

FIGURE 8. Theoretical prediction (5) and measured S_{11}, S_{21} and group-delay parameter performances for the manufactured prototype I filter (see Table 1).

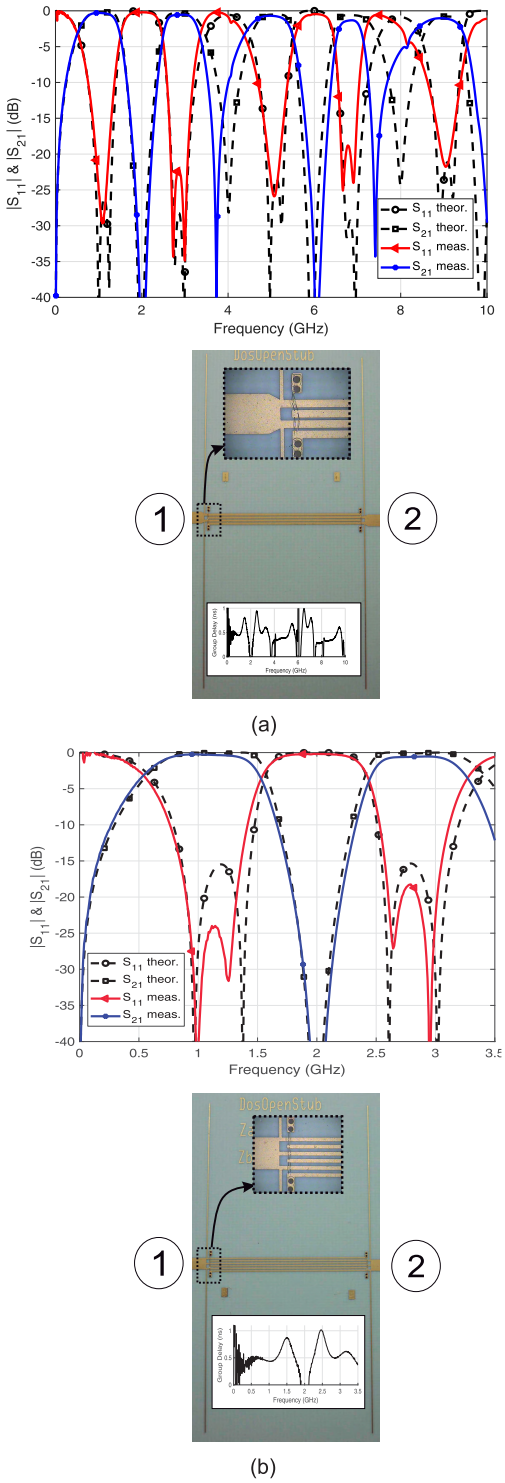

FIGURE 9. Theoretical prediction (6) and measured S_{11}, S_{21} and group-delay parameter performances for the manufactured prototype II filters (see Table 1).

Nevertheless, to achieve high frequency ratios, low stub impedances (Z_{0_b}) must be used. Furthermore, increasing the number of conductors (k) must be taken into account in order to get low MTL impedances (Z_{0_a}) and high coupling factors (c) [27]. Prototype II does not allow narrow bandwidths, because of large stub widths would be needed. In addition, it is remarkable that frequency ratio hardly varies with the

TABLE 1. Physical dimensions of the fabricated filters.

	f_0 (GHz)	FBW* (%)	f_{02}/f_{01}	Z_{0_a} (Ω)	Z_{0_b} (Ω)	c (dB)	Z_{sc_a} (Ω)	Z_{oe_a} (Ω)	Z_{oo_a} (Ω)	k_a	W_a (μm)	S_a (μm)	l_a (mm)	W_b (μm)	l_b (mm)
Fig. 8	3.5	30	2.2	90	80	-5	115	184	78	4	180	214	12	685	12
Fig. 9(a)	2	30	2.55	60	70	-4	102.5	157	57	4	314	118	23.5	130	23.8
Fig. 9(b)	2	48	2.45	50	70	-4	85	185	75	6	195	200	23.7	130	24

FBW*: 3 dB-Fractional Bandwidth (Prototype I) or Fractional Bandwidth with equal-ripple response (Prototype II)

TABLE 2. Comparison among the proposed dual-band filters and published ones.

Filter	Frequency ratio (f_{02}/f_{01})	3-dB FBW (%)	Return Losses (dB)	Insertion Losses (dB)	Transmission Zeros in (0, $2f_0$)	Size ($\lambda_g \times \lambda_g$)
[9]	1.08	4 / 3.7	21.52 /23.78	0.98 / 1.03	2	$0.33\lambda_g \times 0.34\lambda_g$
[11]	1.41	13 / 9.3	12	1.2	4	$0.3\lambda_g \times 0.28\lambda_g$
[35]	2.24	6.5 / 19.1	15 / 12	1.86 / 1.4	3	$0.327\lambda_g \times 0.194\lambda_g$
[36] A	1.77	3.3 / 2.4	14	1.3 / 1.8	3	$0.29\lambda_g \times 0.58\lambda_g$
[36] B	1.97	8.2 / 6.7	14	1.3 / 1.2	4	$0.29\lambda_g \times 0.29\lambda_g$
Fig. 8	2.2	30	24.9 / 27.2	0.6 / 0.74	3	$0.36\lambda_g \times 0.18\lambda_g$
Fig. 9(a)	2.55	48	29.7 / 22	0.28 / 0.54	3	$0.165\lambda_g \times 0.33\lambda_g$
Fig. 9(b)	2.45	50	24 / 18.5	0.25 / 0.52	3	$0.17\lambda_g \times 0.34\lambda_g$

MTL impedance. As this impedance must be low, the number of conductors has to be increased to achieve the desired MTL impedances [27], justifying again the use of multiconductor transmission lines instead of only a pair of coupled lines. Thus, prototype I is more appropriate when using higher frequency ratios and narrow bandwidths, whereas prototype II is better suited to wide bandwidths. Once these criteria are taken into account, the design parameters can be effortlessly selected to synthesize the desirable frequency response of the filter.

Taking into account the design considerations and limitations previously mentioned, it is possible to elaborate a design procedure to select the best prototype depending on the required specifications. This procedure can be summarized as follows.

- *Step 1:* From (8), calculate θ_{01} and θ_{02} according to the desired central frequencies of both bands (f_{01}, f_{02}) and the fractional bandwidth (FBW). Obtain the value of f_0.
- *Step 2:* Choose the MTLs and stubs lengths to be a quarter-wavelength long at f_0.
- *Step 3:* Obtain the values of a and b using (9).
- *Step 4:* Look at Figs. 4 and 5 and decide which prototype is more suitable for the given specifications, taking into account the fractional bandwidth definition. When choosing the first prototype, consider $L_R = 3$ dB ($\epsilon = 1$), but for the second one, obtain the in-band ripple factor ϵ, depending on the desired return losses L_R (12).
- *Step 5:* Use (19) or (22) and (24), depending on the chosen prototype, to calculate the required values of Z_{0_a}, c and Z_{0_b}.

Finally, verify that the accomplished values are physically achievable by the manufacturing process.

IV. EXPERIMENTAL VALIDATION

In order to assess the developed theory and techniques, three filters have been designed, fabricated and measured. For prototype I, the center frequency was $f_0 = 3.9$ GHz, using the analytical equation (19) to choose its parameters. For the two filters of prototype II, the center frequency was set to be $f_0 = 2$ GHz, using (22a), (22b) and (23). The physical dimensions and design parameters are given in Table 1. All the measurements have been obtained by using Agilent N5247A PNA-X, after a TRL calibration to position reference planes correctly for further comparisons. Figure 7 details the coaxial to microstrip transition used for the characterization of filters designed in this paper. Figures 8 and 9 show the predicted values by analytical equations (5) and (6) and measured S-parameter results of the fabricated prototypes. In this sense, the measured group delay responses and photographs of these filters are depicted as well in Figs. 8 and 9. For prototype II, double shunt open stubs has been used, in order to reduce the stub width. The minimum strip width and gap between lines allowed by our manufacturing capability is limited to 100 μm, which determines the range of possible values of Z_{0_a}, Z_{0_b} and c, and therefore, conditions the achievable frequency responses of the filters.

From Figs. 8 and 9, it is noted that there is a very good agreement between the predicted and measured S-parameter results. In Fig. 9(a), it is plotted the broad-band measurement of one of the filters. As they are distributed structures, there will be replicas because of the wavelength dependence. The selectivity at the high side of the first passband and the low side of the second passband is better because they are close to the transmission zero, whereas in the opposite sides of the passband, transmission zeros are far away and the slope is slight. Fractional bandwidth of 30% is used in the filter of the first prototype, whereas 30% and 48% are the ones for the second type. Deviations in the central frequency f_0 or S_{11} parameters and high-frequency degradation are mainly due to fabrication tolerances, unequal even- and odd-mode phase velocities in the wire-bonded MTLs as well as tee junction and open-ended effect in the shunt stubs [34].

Finally, a comparison of the proposed prototypes is summarized in Table 2. In this table, 3-dB FBW is used in all the cases, and λ_g denotes the guided wavelength at center frequency of the lower passband. The proposed filters are more compact even taking into account that stubs are not bent, which would have reduced even more the size of the circuits in the transversal dimension. In terms of insertion and return losses, the obtained results are significant in both bands, outperforming most of the compared cases. It must be taken into account that all the filters have been designed directly using the computed analytical equations previously developed, without any optimization made by an electromagnetic simulator. Furthermore, it is important to remark that there was no post-manufacture tuning. These facts are really significant not only for validating the presented theory, but also for providing feasibility in order to design dual-band bandpass filters without using an EM simulator, just by taking the analytical equations developed and calculating the MTL and stub parameters [37], [38].

V. CONCLUSION

In this work, a rigorous analytical study consisting of short-circuited wire-bonded multiconductor transmission lines and shunt open stubs has been performed to design dual-band bandpass filters. First, closed-form equations are presented to characterize the behavior of the two developed configurations. From these analytical equations, a synthesis procedure is carried out to obtain the parameters that enable to have a desired Chebyshev frequency response. Expressions for two configurations, single-stub with two MTL sections and double-stub with a MTL section filters, have been deduced and validated through experimental results. In addition, the formulas presented here are also suited for designing other double-band bandpass coupled-line based filters. Finally, it is important to stand out the excellent agreement between measured results and theoretical predictions, which gives designers an useful mathematical tool based on the developed theory for a quick and accurate synthesis of dual-band bandpass filters.

APPENDIX A
FILTERING FUNCTIONS FOR PROTOTYPE I

Given the prescribed transmission zeros in the low-pass domain as

$$\omega_z = \{0, \infty, j, -j\} \tag{25}$$

the filtering function in the normalized frequency ω for a fourth-order Chebyshev filter is obtained as follows [31]

$$F_I(\omega) = \frac{t_4\omega^4 + t_2\omega^2 + t_0}{\omega\left(\delta^2 + \omega^2\right)}. \tag{26}$$

This function is mapped to the θ-plane as ($\omega = -\delta \cot\theta$)

$$F_n(\theta) = \frac{g_{4t}\tan^4\theta + g_{2t}\tan^2\theta + g_{t0}}{\tan\theta\left(1 + \tan^2\theta\right)}, \tag{27}$$

where coefficients t_i and g_{it} are given as

$$\begin{aligned}
t_4 &= K\frac{\gamma(1+\omega_1)+2}{(1-\omega_1)^2(1+\omega_1)}\\
t_2 &= K\frac{-\gamma(1+\omega_1)(1+\omega_1^2)-(1+\omega_1)^2-S_1(1-\omega_1)^2}{(1-\omega_1)^2(1+\omega_1)}\\
t_0 &= K\frac{\gamma\omega_1^2(1+\omega_1)+\omega_1(1+\omega_1^2+S_1(1-\omega_1^2))}{(1-\omega_1)^2(1+\omega_1)}\\
g_{4t} &= \frac{-t_0}{\delta^3}, \quad g_{2t} = \frac{-t_2}{\delta}, \quad g_{0t} = -t_4\delta\\
K &= \frac{2\delta^2+\omega_1^2+1}{2}, S_1 = \frac{\omega_1^2-1}{4K}, \gamma = \frac{2}{1+\omega_1}\sqrt{1-S_1^2}.
\end{aligned} \tag{28}$$

Equating this filtering function with the transfer function in (5), the following equations are obtained

$$\begin{aligned}
g_2/g_4 &= g_{2t}/g_{4t} = \delta^2 t_2/t_0\\
g_0/g_4 &= g_{0t}/g_{4t} = \delta^4 t_4/t_0.
\end{aligned} \tag{29}$$

From these equations it is easy to derive the design expressions to calculate the values of Z_{0_a} and Z_{0_b} as a function of the coupling factor c as follows

$$\bar{Z}_{0_a}^4 - \frac{g_{2t}(1-c^2)+g_{0t}c^2}{g_{0t}c^2}\bar{Z}_{0_a}^2 + \frac{g_{4t}(1-c^2)}{g_{0t}c^4} = 0 \tag{30a}$$

$$\bar{Z}_{0_b} = \frac{-g_{0t}c^3\bar{Z}_{0_a}^3}{2g_{4t}(1-c^2)}. \tag{30b}$$

APPENDIX B
ANALYTICAL SOLUTION TO THE QUARTIC EQUATION OF PROTOTYPE II

Given the quartic equation

$$a_4x^4 + a_3x^3 + a_2x^2 + a_1x + a_0 = 0 \tag{31}$$

with $a_4 \neq 0$, the four roots are determined as

$$x_1 = -\frac{a_3}{4a_4} - S + \frac{1}{2}\sqrt{-4S^2 - 2p + \frac{q}{S}} \tag{32a}$$

$$x_2 = -\frac{a_3}{4a_4} - S - \frac{1}{2}\sqrt{-4S^2 - 2p + \frac{q}{S}} \tag{32b}$$

$$x_3 = -\frac{a_3}{4a_4} + S + \frac{1}{2}\sqrt{-4S^2 - 2p - \frac{q}{S}} \tag{32c}$$

$$x_4 = -\frac{a_3}{4a_4} + S - \frac{1}{2}\sqrt{-4S^2 - 2p - \frac{q}{S}} \tag{32d}$$

where

$$\begin{aligned}
p &= \frac{8a_4a_2 - 3a_3^2}{8a_4^2}\\
q &= \frac{a_3^3 - 4a_4a_3a_2 + 8a_4^2a_1}{8a_4^3}\\
S &= \frac{1}{2}\sqrt{-\frac{2}{3}p + \frac{1}{3a_4}\left(Q + \frac{\Delta_0}{Q}\right)}
\end{aligned} \tag{33}$$

and where

$$Q = \sqrt[3]{\frac{\Delta_1 + \sqrt{\Delta_1^2 - 4\Delta_0^3}}{2}}$$
$$\Delta_0 = a_2^2 - 3a_3a_1 + 12a_4a_0$$
$$\Delta_1 = 2a_2^3 - 9a_3a_2a_1 + 27a_3^2a_0 + 27a_4a_1^2 - 72a_4a_2a_0. \tag{34}$$

If the discriminant Δ, defined as

$$\Delta = \frac{\Delta_1^2 - 4\Delta_0^3}{-27} \tag{35}$$

is greater that 0, then Q is a complex number, and S must be recalculated as

$$S = \frac{1}{2}\sqrt{-\frac{2}{3}p + \frac{2}{3a_4}\sqrt{\Delta_0}\cos\frac{\phi}{3}} \tag{36}$$

where

$$\phi = \arccos\left(\frac{\Delta_1}{2\sqrt{\Delta_0^3}}\right). \tag{37}$$

It is worthy to mention that, if the value of q is negative, x_1 (32a) must be chosen as the correct solution, but if it is positive, x_3 (32c) will be the chosen solution for the synthesis procedure.

REFERENCES

[1] L. Kong and X. Xu, "A compact dual-band dual-polarized microstrip antenna array for MIMO-SAR applications," *IEEE Trans. Antennas Propag.*, vol. 66, no. 5, pp. 2374–2381, May 2018.

[2] A. Toktas and A. Akdagli, "Compact multiple-input multiple-output antenna with low correlation for ultra-wide-band applications," *IET Microw., Antennas Propag.*, vol. 9, no. 8, pp. 822–829, May 2015.

[3] D. Psychogiou, R. Gómez-García, and D. Peroulis, "Fully adaptive multi-band bandstop filtering sections and their application to multifunctional components," *IEEE Trans. Microw. Theory Techn.*, vol. 64, no. 12, pp. 4405–4418, Dec. 2016.

[4] M. Pal and R. Ghatak, "A distinctive resonance: Multiband bandpass filter design techniques using multimode resonators," *IEEE Microw. Mag.*, vol. 16, no. 11, pp. 36–55, Dec. 2015.

[5] H. Miyake, S. Kitazawa, T. Ishizaki, T. Yamada, and Y. Nagatomi, "A miniaturized monolithic dual band filter using ceramic lamination technique for dual mode portable telephones," in *IEEE MTT-S Int. Microw. Symp. Dig.*, vol. 2, Jun. 1997, pp. 789–792.

[6] L.-C. Tsai and C.-W. Hsue, "Dual-band bandpass filters using equal-length coupled-serial-shunted lines and Z-transform technique," *IEEE Trans. Microw. Theory Techn.*, vol. 52, no. 4, pp. 1111–1117, Apr. 2004.

[7] W. Feng, Y. Zhang, and W. Che, "Tunable dual-band filter and diplexer based on folded open loop ring resonators," *IEEE Trans. Circuits Syst. II, Exp. Briefs*, vol. 64, no. 9, pp. 1047–1051, Sep. 2017.

[8] H. Liu, L. Shen, L. Y. Shi, Y. Jiang, X. Guan, and T. Wu, "Dual-mode dual-band bandpass filters design using open-loop slotline resonators," *IET Microw., Antennas Propag.*, vol. 7, no. 12, pp. 1027–1034, Sep. 2013.

[9] V. Rathore, S. Awasthi, and A. Biswas, "Design of compact dual-band bandpass filter using frequency transformation and its implementation with split ring resonator dual-band bandpass filter using SRR," in *Proc. 44th Eur. Microw. Conf.*, Oct. 2014, pp. 949–952.

[10] B. Ren *et al.*, "Compact dual-band differential bandpass filter using quadruple-mode stepped-impedance square ring loaded resonators," *IEEE Access*, vol. 6, pp. 21850–21858, Apr. 2018.

[11] H. Zhu and A. M. Abbosh, "Single- and dual-band bandpass filters using coupled stepped-impedance resonators with embedded coupled-lines," *IEEE Microw. Wireless Compon. Lett.*, vol. 26, no. 9, pp. 675–677, Sep. 2016.

[12] W. Jiang, W. Shen, T. Wang, Y. M. Huang, Y. Peng, and G. Wang, "Compact dual-band filter using open/short stub loaded stepped impedance resonators (OSLSIRs/SSLSIRs)," *IEEE Microw. Wireless Compon. Lett.*, vol. 26, no. 9, pp. 672–674, Sep. 2016.

[13] H. Liu, B. Ren, X. Guan, J. Lei, and S. Li, "Compact dual-band bandpass filter using quadruple-mode square ring loaded resonator (SRLR)," *IEEE Microw. Wireless Compon. Lett.*, vol. 23, no. 4, pp. 181–183, Apr. 2013.

[14] H.-Y. A. Yim and K.-K. M. Cheng, "Novel dual-band planar resonator and admittance inverter for filter design and applications," in *IEEE MTT-S Int. Microw. Symp. Dig.*, Jun. 2005, pp. 1–4.

[15] J. Ha and Y. Lee, "Dual-band filter with fully independent passbands based on unequal-length coupled lines and stubs," *IET Microw., Antennas Propag.*, vol. 11, no. 15, pp. 2141–2147, Dec. 2017.

[16] C.-W. Tang, S.-F. You, and I.-C. Liu, "Design of a dual-band bandpass filter with low-temperature co-fired ceramic technology," *IEEE Trans. Microw. Theory Techn.*, vol. 54, no. 8, pp. 3327–3332, Aug. 2006.

[17] S. Y. Zheng, Z. L. Su, Y. M. Pan, Z. Qamar, and D. Ho, "New dual-/tri-band bandpass filters and diplexer with large frequency ratio," *IEEE Trans. Microw. Theory Techn.*, vol. 66, no. 6, pp. 2978–2992, Jun. 2018.

[18] A. García-Lampérez and M. Salazar-Palma, "Single-band to multiband frequency transformation for multiband filters," *IEEE Trans. Microw. Theory Techn.*, vol. 59, no. 12, pp. 3048–3058, Dec. 2011.

[19] M. Pérez-Escribano, J. J. Sánchez-Martínez, and E. Márquez-Segura, "Small size dual-band bandpass filters with multiconductor transmission lines and shunt open stubs," in *Proc. 48th Eur. Microw. Conf.*, Sep. 2018, pp. 962–965.

[20] R. Li, S. Sun, and L. Zhu, "Synthesis design of ultra-wideband bandpass filters with composite series and shunt stubs," *IEEE Trans. Microw. Theory Techn.*, vol. 57, no. 3, pp. 684–692, Mar. 2009.

[21] J.-Y. Li, C.-H. Chi, and C.-Y. Chang, "Synthesis and design of generalized Chebyshev wideband hybrid ring based bandpass filters with a controllable transmission zero pair," *IEEE Trans. Microw. Theory Techn.*, vol. 58, no. 12, pp. 3720–3731, Dec. 2010.

[22] R. Zhang and L. Zhu, "Synthesis and design of wideband dual-band bandpass filters with controllable in-band ripple factor and dual-band isolation," *IEEE Trans. Microw. Theory Techn.*, vol. 61, no. 5, pp. 1820–1828, May 2013.

[23] R. Zhang and L. Zhu, "Synthesis of dual-wideband bandpass filters with source-load coupling network," *IEEE Trans. Microw. Theory Techn.*, vol. 62, no. 3, pp. 441–449, Mar. 2014.

[24] I. Hunter, *Theory and Design of Microwave Filters*. Stevenage, U.K.: IEEE Press, 2001.

[25] J. J. Sánchez-Martínez and E. Márquez-Segura, "Analysis of wire-bonded multiconductor transmission line-based phase-shifting sections," *J. Electromagn. Waves Appl.*, vol. 27, no. 16, pp. 1997–2009, Sep. 2013.

[26] W. P. Ou, "Design equations for an interdigitated directional coupler (short papers)," *IEEE Trans. Microw. Theory Techn.*, vol. MTT-23, no. 2, pp. 253–255, Feb. 1975.

[27] J. J. Sánchez-Martínez and E. Márquez-Segura, "Analytical design of wire-bonded multiconductor transmission-line-based ultra-wideband differential bandpass filters," *IEEE Trans. Microw. Theory Techn.*, vol. 62, no. 10, pp. 2308–2315, Oct. 2014.

[28] G. L. Mattahei, E. M. T. Jones, and L. Young, *Microwave Filters, Impedance-Matching Networks, and Coupling Structures*. Norwood, MA, USA: Artech House, 1985.

[29] R. J. Cameron, "General coupling matrix synthesis methods for Chebyshev filtering functions," *IEEE Trans. Microw. Theory Techn.*, vol. 47, no. 4, pp. 433–442, Apr. 1999.

[30] G. Macchiarella and S. Tamiazzo, "Design techniques for dual-passband filters," *IEEE Trans. Microw. Theory Techn.*, vol. 53, no. 11, pp. 3265–3271, Nov. 2005.

[31] S. Amari, F. Seyfert, and M. Bekheit, "Theory of coupled resonator microwave bandpass filters of arbitrary bandwidth," *IEEE Trans. Microw. Theory Techn.*, vol. 58, no. 8, pp. 2188–2203, Aug. 2010.

[32] J.-S. Hong and M. J. Lancaster, *Microstrip Filters for RF/Microwave Applications*, K. Chang, Ed. Hoboken, NJ, USA: Wiley, 2001.

[33] M. Mahmood, S. Hammad, and I. Mahmood, "An efficient algorithm for computing the roots of general quadratic, cubic and quartic equations," *Int. J. Math. Educ. Sci. Technol.*, vol. 45, no. 7, pp. 1095–1103, Apr. 2014.

[34] M. Kirschning, R. H. Jansen, and N. H. L. Koster, "Accurate model for open end effect of microstrip lines," *Electron. Lett.*, vol. 17, no. 3, pp. 123–125, Feb. 1981.

[35] Y.-H. Lo, L.-J. Chen, and K.-H. Lin, "Design of dual-band bandpass filter using stub-loaded resonator with source-load coupling and spur-line at 2.45/5.5 GHz for WLAN applications," in *Proc. IEEE Int. Workshop Electromagn. (iWEM)*, Aug. 2014, pp. 193–194.

[36] H. Zhang, W. Kang, and W. Wu, "Miniaturized dual-band SIW filters using E-shaped slotlines with controllable center frequencies," *IEEE Microw. Wireless Compon. Lett.*, vol. 28, no. 4, pp. 311–313, Apr. 2018.

[37] M. Kirschning and R. H. Jansen, "Accurate wide-range design equations for the frequency-dependent characteristic of parallel coupled microstrip lines," *IEEE Trans. Microw. Theory Techn.*, vol. MTT-32, no. 1, pp. 83–90, Jan. 1984.

[38] R. H. Jansen and M. Kirschning, "Arguments and an accurate model for the power-current formulation of microstrip characteristic impedance," *AEU*, vol. 37, nos. 3–4, pp. 108–112, Mar./Apr. 1983.

JUAN JOSÉ SÁNCHEZ-MARTÍNEZ received the B.S., M.S., and Ph.D. degrees in telecommunication engineering from the University of Málaga, Málaga, Spain, in 2003, 2006, and 2014, respectively.

From 2006 to 2014, he was a Research Assistant with the Department of Communication Engineering, University of Málaga. He was involved in signal processing for digital communications and real-time implementation of signal processing algorithms on field-programmable gate array, until 2010. From 2010 to 2014, he focused on the analysis of planar structures and the design of microwave passive devices. In 2014, he joined Indra Sistemas, Spain, where he is involved in different projects related with electronic warfare. His main tasks are focused on the analysis, design, and development of electronic measures and electronic countermeasures systems for air and naval applications, including the design of wideband cavity backed spiral antennas, passive and active circuits, and wideband and high-power GaN amplifiers.

In 2012, he joined the Department of Electrical and Electronic Engineering, Imperial College London, London, U.K., as a Visiting Scholar. He was a recipient of the Junta de Andalucía Scholarship, from 2010 to 2014.

MARIO PÉREZ-ESCRIBANO was born in Alcalá la Real, Jaén, Spain, in 1993. He received the B.S. degree in telecommunication engineering from the University of Málaga, Málaga, Spain, in 2015, and the M.S. degree in telecommunication engineering from the University Carlos III de Madrid, Madrid, Spain, in 2017.

In 2014, he joined the Departamento de Ingeniería de Comunicaciones, Escuela Técnica Superior de Ingeniería (ETSI) de Telecomunicación, Universidad de Málaga, Málaga, Spain, where he is currently pursuing the Ph.D. degree. His research interests include the analysis of structures made by additive manufacturing techniques, planar circuits, and dielectric resonator antennas.

Mr. Pérez-Escribano was a recipient of the Spanish Ministry of Education, Culture and Sports Scholarship, from 2017 to 2021.

ENRIQUE MÁRQUEZ-SEGURA (S'93–M'95–SM'06) was born in Málaga, Spain, in 1970. He received the Ingeniero de Telecomunicación and Doctor Ingeniero degrees from the Universidad de Málaga, Málaga, in 1993 and 1998, respectively.

In 1994, he joined the Departamento de Ingeniería de Comunicaciones, Escuela Técnica Superior de Ingeniería de Telecomunicación, Universidad de Málaga, where he became an Associate Professor, in 2001. His current research interests include electromagnetic material characterization, additive manufacturing, measurement techniques, and RF, microwave, and millimeter-wave circuits design for communication applications.

Dr. Márquez-Segura was a recipient of the Spanish Ministry of Education and Science Scholarship, from 1994 to 1995.